



ORIGINAL ARTICLE

# Physicochemical characterization and *in vitro* dissolution studies of solid dispersions of ketoprofen with PVP K30 and D-mannitol

Pankajkumar S. Yadav <sup>a,\*</sup>, Vikas Kumar <sup>a</sup>, Udaya Pratap Singh <sup>a</sup>,  
Hans Raj Bhat <sup>a</sup>, B. Mazumder <sup>b</sup>

<sup>a</sup> Department of Pharmaceutical Sciences, Sam Higginbottom Institute of Agriculture, Technology and Sciences, Allahabad 211 007, Uttar Pradesh, India

<sup>b</sup> Department of Pharmaceutical Sciences, Dibrugarh University, Dibrugarh 786 004, Assam, India

Received 30 September 2011; accepted 17 December 2011

Available online 24 December 2011

## KEYWORDS

Ketoprofen;  
Solid dispersion;  
PVP K30;  
D-Mannitol;  
Kneading;  
Melting;  
Solvent evaporation

**Abstract** Aim of the present study was to improve the solubility and dissolution rate of poorly water soluble, BCS class-II drug Ketoprofen (KETO) by solid-dispersion approach. Solid dispersions were prepared by using polyvinylpyrrolidone K30 (PVP K30) and D-mannitol in different drugs to carrier ratios. Dispersions with PVP K30 were prepared by kneading and solvent evaporation techniques, whereas solid dispersions containing D-mannitol were prepared by kneading and melting techniques. These formulations were characterized in the liquid state by phase-solubility studies and in the solid state by Differential Scanning Calorimetry (DSC), Fourier Transform Infrared (FTIR) spectroscopy, X-ray diffraction (XRD) and Scanning Electron Microscopy (SEM). The aqueous solubility of KETO was favored by the presence of both carriers. The negative values of Gibbs free energy illustrate the spontaneous transfer from pure water to the aqueous polymer environment. Solid state characterization indicated KETO was present as fine particles in D-mannitol solid dispersions and entrapped in carrier matrix of PVP K30 solid dispersions. In contrast to the very slow dissolution rate of pure KETO, dispersions of drug in carriers considerably improved the dissolution rate. This can be attributed to increased wettability and dispersibility, as well as decreased crystallinity and increase in amorphous fraction of drug. Solid dispersions prepared with PVP K30 showed the highest improvement in dissolution rate of KETO. Even physical mixtures of KETO prepared with both carriers also showed better dissolution profiles than those of pure KETO.

© 2011 King Saud University. Production and hosting by Elsevier B.V. All rights reserved.

\* Corresponding author. Tel.: +91 9208474935; fax: +91 532 2684394.

E-mail address: pypharm@gmail.com (P.S. Yadav).

Peer review under responsibility of King Saud University.



Production and hosting by Elsevier

## 1. Introduction

Poorly water-soluble drugs are associated with slow drug absorption leading eventually to inadequate and variable bio-availability (Amidon et al., 1995; Leuner and Dressman, 2000). Nearly 40% of the new chemical entities currently being discovered are poorly water-soluble drugs (Lipinski, 2002; Hu

et al., 2004). Based upon their permeability characteristics, the Biopharmaceutical Classification System (BCS) categorizes such drugs into two major classes, viz. Class II and IV (Amidon et al., 1995; <http://www.fda.gov/downloads/Drugs/Guidance-ComplianceRegulatoryInformation/Guidances/ucm070246.pdf>). The BCS class II drugs encompass poorly water-soluble entities with high permeability. Attempts to enhance drug solubility of these therapeutic agents correlate well with enhancement in their bioavailability (Amidon et al., 1995; Leuner and Dressman, 2000; <http://www.fda.gov/downloads/Drugs/Guidance-ComplianceRegulatoryInformation/Guidances/ucm070246.pdf>). Most formulation strategies for such drugs are targeted at enhancing their dissolution rate and/or solubility by achieving their fine dispersion at absorption level (Leuner and Dressman, 2000; Wyatt, 1999; Craig, 1993). This can be attained by formulating supersaturated systems (i.e., solid dispersion) of the drug employing diverse types of carriers, ranging widely from water-soluble to amphiphilic to lipid-soluble ones (Leuner and Dressman, 2000; Habib, 2001; Serajuddin, 1999; Charman, 2000). Solid dispersion is a group of solid product consisting, generally, a hydrophobic drug and hydrophilic matrix. This approach is useful for the improvement of solubility of poorly soluble drugs.

Ketoprofen is Non-Steroidal Anti-Inflammatory Drug (NSAID) of propionic acid class having analgesic and anti pyretic effects. In BCS, it is categorized in Class II (<http://www.tsrlinc.com/resources/services/>). Solid-dispersion strategy has been experimented for KETO, and various carriers have been tested (Margarit et al., 1994; Roger and Anderson, 1982; Sheen et al., 1995; Takayama et al., 1982). Here authors have formulated solid dispersions of KETO with some more carriers (i.e., PVP K30 and D-mannitol) by various methods with the objective to improve the solubility of the same.

## 2. Materials and methods

### 2.1. Materials

For preparation of solid dispersions the following materials were used: Ketoprofen (Gift sample from Alembic Pvt. Ltd., India); polyvinylpyrrolidone K30 (Gift sample from Sun Pharmaceutical Industries, India); D-(-) Mannitol Extra pure (Loba Chemie Indoaustranal Co., India). Analytical grade of solvents were used.

### 2.2. Phase solubility studies

Phase-solubility studies were carried out by adding excess of drug (60 mg) in 25 ml of aqueous solution of different (5%, 10%, 15% and 20%) PVP or D-mannitol concentrations. The suspensions were continuously stirred on an electromagnetic stirrer with a hot plate (Remi, India) at 37 °C and 300 rpm for 48 h (this duration was previously tested to be sufficient to reach equilibrium). The suspensions were filtered through a 0.22 µm nylon membrane filter. The filtrates were suitably diluted and analyzed, spectrophotometrically (UV-1700, UV/Vis spectrophotometer, Shimadzu, Japan), for the dissolved drug at 259 nm. All assays were performed in triplicate.

The Gibbs free energy of transfer ( $\Delta G_{tr}^0$ ) of KETO from pure water to the aqueous solution of carrier was calculated as follows:

$$\Delta G_{tr}^0 = -2.303RT \log S_0/S_S$$

where  $S_0/S_S$  is the ratio of molar solubility of KETO in aqueous solutions of carrier to that of the same medium without carrier.

1:1 complex apparent stability constant ( $K_a$ ) was determined as follows:

$$K_a = \frac{\text{Slope}}{\text{Intercept}(1 - \text{Slope})}$$

where slope and intercept were obtained from the graph of %w/v of ketoprofen vs. aqueous concentration of carrier (PVP K30 and D-mannitol) in %w/v.

### 2.3. Preparation of solid dispersion

Solid dispersions were prepared by three different methods and were compared with the drug carrier physical mixture and pure KETO.

#### 2.3.1. Melting method

Three solid-dispersion preparations containing different weight ratios of KETO in D-mannitol (1:1, 1:3, 1:5, and denoted as MMDM 1:1, 1:3, 1:5, respectively) were prepared by the melting method. KETO was added to the melted D-mannitol at 168 °C, and the resulting homogeneous preparation was rapidly cooled in a freezing mixture of ice and sodium chloride and stored in a desiccator for 24 h. Subsequently, the dispersion was ground in a mortar and sieved through 60# sieve. The resulted product was stored in a desiccator until further evaluation.

#### 2.3.2. Solvent evaporation method

Solid dispersions of KETO in PVP K30 containing different weight ratios (1:1, 1:3, 1:5 and denoted as SMPVP 1:1, 1:3, 1:5, respectively) were prepared by the solvent evaporation method as follows. To a solution of weighed quantity of KETO in a minimum amount of ethanol, the appropriate amount of PVP K30 was added. The resulting mixture was stirred for 1 h and evaporated at a temperature of 45–50 °C on water bath until nearly dry and then stored in a desiccator over anhydrous CaCl<sub>2</sub>, to constant weight. The evaporated product was ground in a mortar and passed through a sieve 60# and stored in a desiccator until further evaluation.

#### 2.3.3. Kneading method

Solid Dispersions of KETO in PVP K30 in different weight ratios (1:1, 1:3, 1:5 and denoted as KMPVP 1:1, 1:3, 1:5, respectively) and D-mannitol in different weight ratios (1:1, 1:3, 1:5 and denoted as KMDM 1:1, 1:3, 1:5, respectively) were prepared by the kneading method as follows. A mixture of PVP K30 and KETO was wetted with water and kneaded thoroughly for 30 min in a glass mortar. The paste formed was dried for 24 h. Dried powder was passed through 60# sieve and stored in a desiccator until further evaluation.

#### 2.3.4. Physical mixtures

Physical mixtures having the same weight ratios were prepared by thoroughly mixing appropriate amounts of KETO and PVP

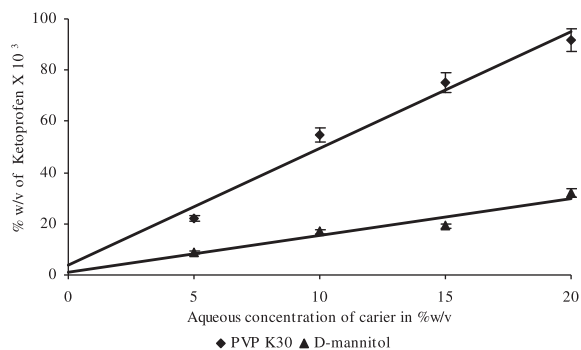


**Figure 1** Solubility of KETO (g/100 ml) in aqueous solutions of PVP K30 and D-mannitol in water at 37 °C. (Each point represents mean of three determinations.)

**Table 1** Gibbs free energy values and apparent stability constants ( $K_a$ ) of KETO-PVP K30 and KETO-D-mannitol interactions.

Concentration (% w/v)	$\Delta G_{tr}^0$ (kJ/mol)	
	PVP K30	D-mannitol
5	-22.18	-19.77
10	-24.52	-21.51
15	-25.33	-21.81
20	-25.84	-23.13
Intercept	$1.51 \times 10^{-4}$	$4.91 \times 10^{-5}$
Slope	$1.79 \times 10^{-2}$	$5.66 \times 10^{-3}$
$K_a$	120.87	115.85

K30 in different weight ratios (1:1, 1:3, 1:5 and denoted as PMPVP 1:1, 1:3, 1:5, respectively) and D-mannitol in different weight ratios (1:1, 1:3, 1:5 and denoted as PMDM 1:1, 1:3, 1:5, respectively) in a mortar until a homogeneous mixture was obtained. The resulting mixtures were sieved through a 60# sieve. The resulted product was stored in a desiccator until further evaluation.

#### 2.4. Characterization of solid dispersion

##### 2.4.1. Fourier Transform Infrared Spectroscopy (FTIR)

FTIR spectra of powder samples were obtained by using a spectrophotometer (Shimadzu, 8400) by potassium bromide (KBr) pellet method (2 mg of sample in 200 mg of KBr). The scanning range was  $650\text{--}3800\text{ cm}^{-1}$  and the resolution was  $2\text{ cm}^{-1}$ .

##### 2.4.2. X-ray diffraction (XRD)

Powder XRD patterns were traced employing X-ray diffractometer (Philips PW 1830, The Netherlands) for the samples, using Ni filtered  $\text{CuK}\alpha$  radiation of wavelength  $1.5404\text{ \AA}$ , a voltage of 35 kV, a current of 30 mA and receiving slit of 0.1 mm. The samples were analyzed over  $2\theta$  range of  $4\text{--}40^\circ$  with a scan step size of  $0.05^\circ$  and a scan step time of 1 s and a scanning rate of  $4^\circ/\text{min}$ .

##### 2.4.3. Differential scanning calorimetry (DSC)

DSC scans of the powdered samples were recorded by using Jade DSC Perkin Elmer, USA. All samples were weighed (8–10 mg) and heated at a scanning rate of  $10^\circ\text{C}/\text{min}$  under dry

nitrogen flow (20 ml/min) between 50 and  $300^\circ\text{C}$ . Aluminum pans and lids were used for all samples. Pure water and indium were used to calibrate the DSC temperature scale and enthalpic response.

##### 2.4.4. Scanning electron microscopy (SEM)

The SEM analysis was carried out using a scanning electron microscope (Hitachi S-3600 N, Japan). Prior to examination, samples were mounted on an aluminum stub using a double sided adhesive tape and then making it electrically conductive by coating with a thin layer of gold (approximately 20 nm) in vacuum. The scanning electron microscope was operated at an acceleration voltage of 15 kV.

#### 2.5. *In vitro* dissolution study

*In vitro* dissolution studies were carried out for pure drug and all products in USP type II dissolution test apparatus (Campbell Electronics, India) at 50 RPM in 900 ml of 0.1M HCl. Fifty milligrams of pure drug and an equivalent amount of solid dispersion were used for the dissolution studies. One milliliter of the aliquot was withdrawn at predetermined intervals and filtered using  $0.22\text{ }\mu\text{m}$  nylon membrane (Pall Life Sciences, India). The required dilutions were made with 0.1 M HCl and

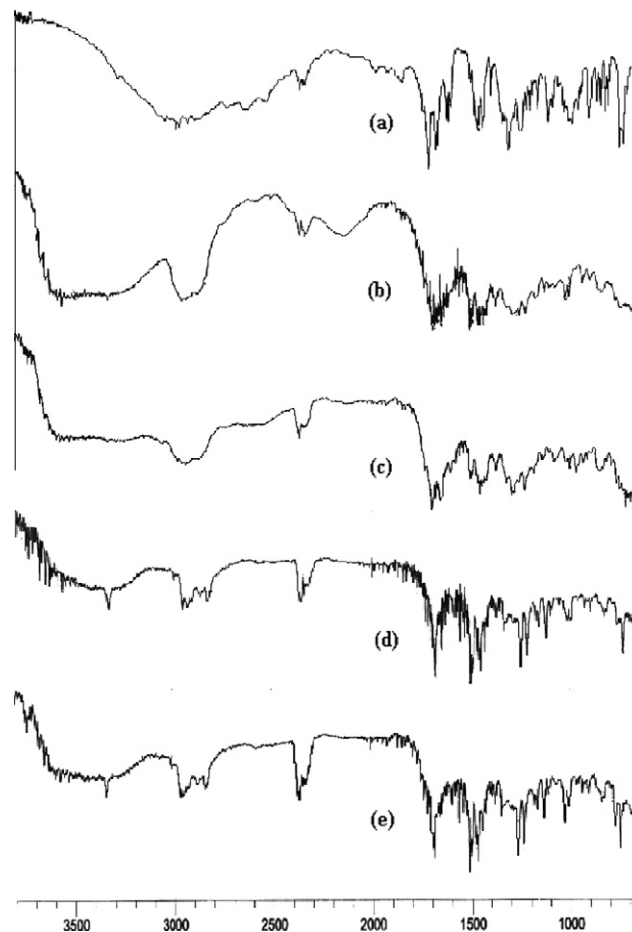


**Figure 2** Comparative study of the FTIR spectra of (a) pure drug KETO; (b) PVP K30; (c) PMPVP 1:5; (d) KMPVP 1:5 and (e) SMPVP 1:5.

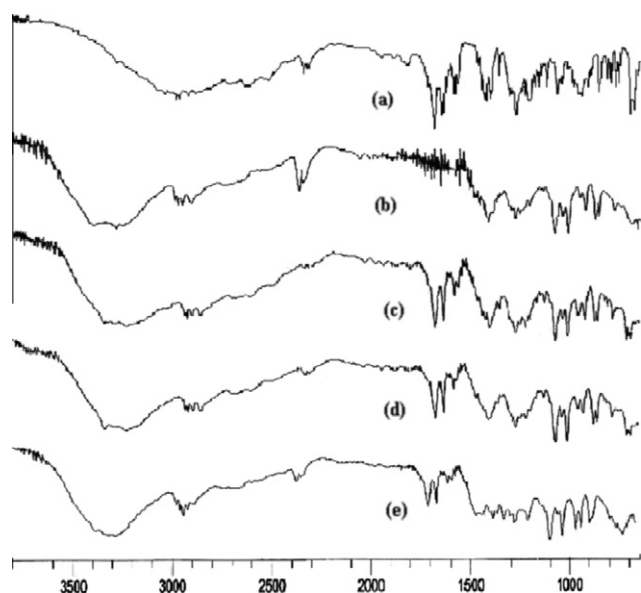


**Figure 3** FTIR spectra of (a) pure drug KETO; (b) D-mannitol; (c) PMDM 1:5; (d) KMDM 1:5 and (e) MMDM 1:5.

the solution was analyzed for the drug content UV spectrophotometrically at 259 nm against 0.1 M HCl. An equal volume of the dissolution medium was replaced in the vessel after each withdrawal to maintain the sink condition. Three determinations were carried out for each formulation. From this, cumulative % of drug dissolved was calculated and plotted against function of time to study the pattern of drug release. Each test was performed in triplicate ( $n = 3$ ), and calculated mean values of cumulative drug release were used while plotting the release curves.  $DP_{30 \text{ min}}$  (drug dissolved within 30 min) values for release of KETO from different samples were calculated.

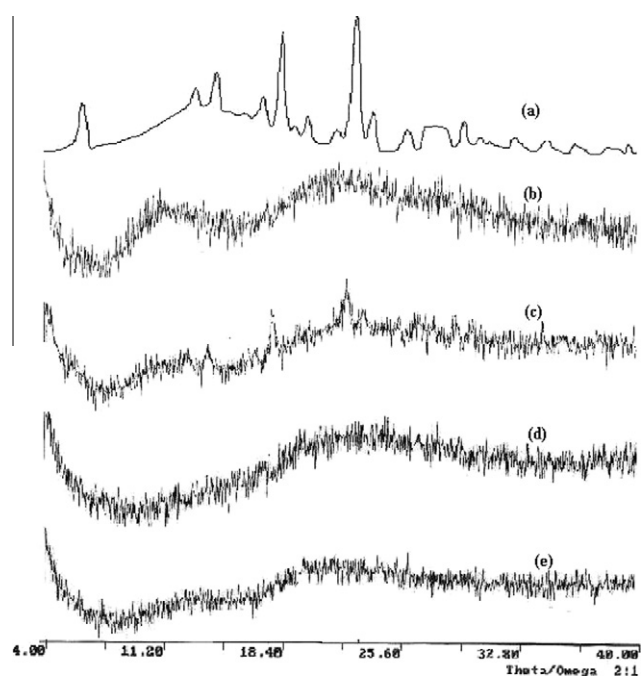


**Figure 4** Powder X-ray diffractograms of (a) pure drug KETO; (b) PVP K30; (c) PMPVP 1:5; (d) KMPVP 1:5 and (e) SMPVP 1:5.

## 2.6. Statistical analysis

For comparison between dissolution profiles of different samples, an independent mathematical approach model for calculating a similarity factor  $f_2$  proposed by Moore and Flanner (1996) was used. The similarity factor  $f_2$  is a measure of similarity in the percentage dissolution between two dissolution curves and is defined by the following equation:

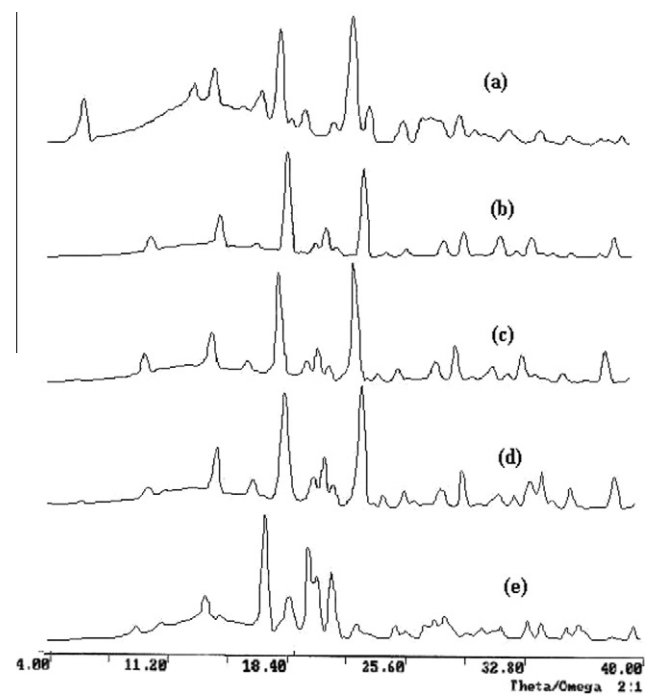
$$f_2 = 50 \times \log \left[ \left\{ 1 + \left( \frac{1}{n} \right) \sum_{i=1}^n w_i (R_i - T_i)^2 \right\}^{-0.5} \right] \times 100$$

where  $n$  is the number of withdrawal points,  $R_i$  is the percentage dissolved of reference at time point  $t$ , and  $T_i$  is the percentage dissolved of test at time point  $t$ . A value of 100% for the similarity factor ( $f_2$ ) suggests that the test and reference profiles are identical. Values between 50 and 100 indicate that the dissolution profiles are similar, whereas smaller values imply an increase in dissimilarity between release profiles. CDER/FDA (<http://www.fda.gov/downloads/Drugs/GuidanceComplianceRegulatoryInformation/Guidances/ucm070237.pdf>) suggests this analysis for an immediate release of solid oral dosage forms.

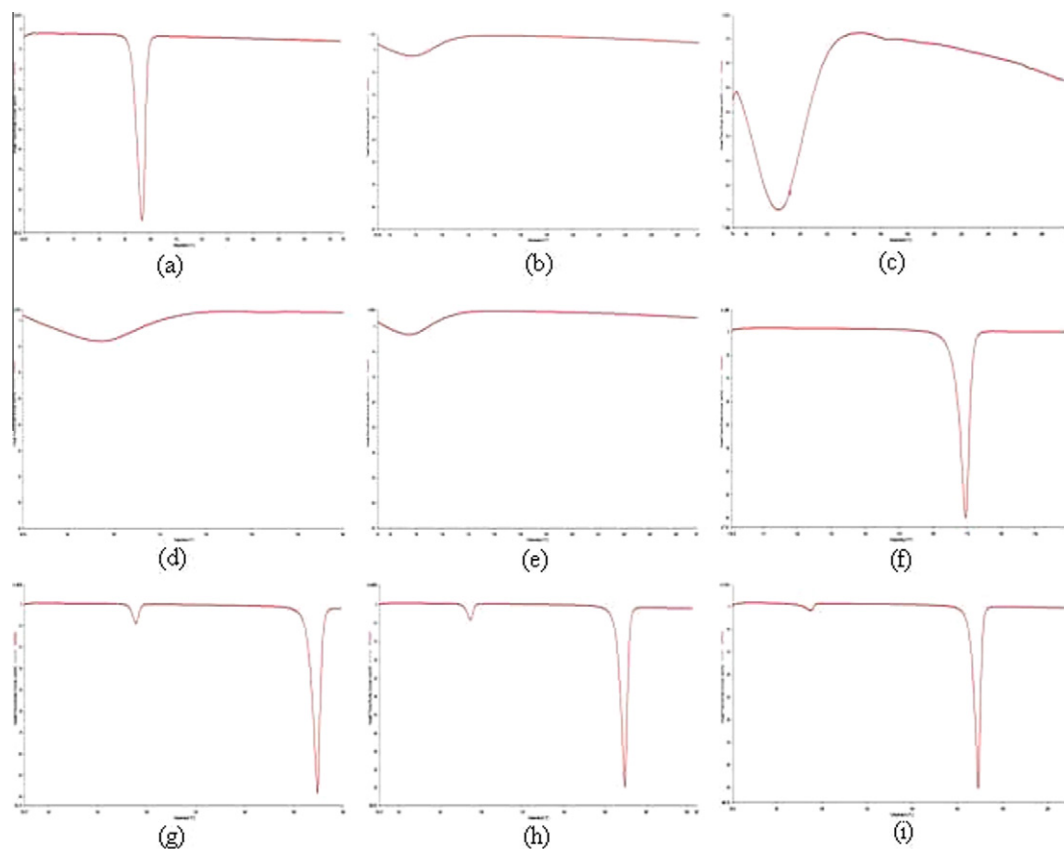
## 3. Results and discussion

### 3.1. Phase solubility studies

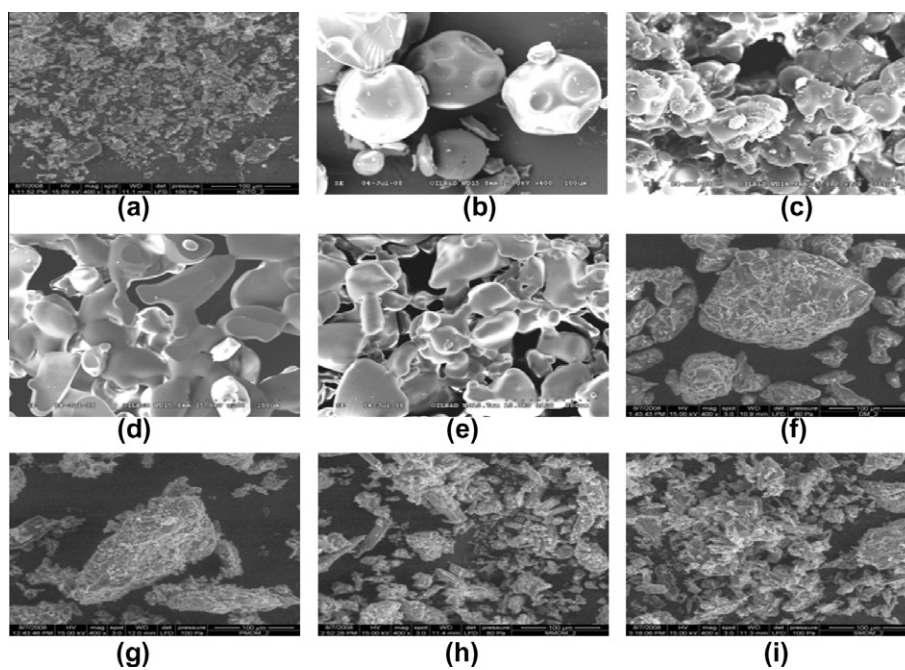
Fig. 1 represents solubility of KETO in the presence of PVP K30 and D-mannitol. The Gibbs free energy of transfer ( $\Delta G_{tr}^0$ ) and apparent stability constants ( $K_a$ ) derived from Fig. 1 are shown in Table 1. The plots of drug solubility against the polymer concentration (Fig. 1) indicate a linear



**Figure 5** Powder XRD spectra of (a) pure drug KETO; (b) D-mannitol; (c) PMDM 1:5; (d) KMDM 1:5 and (e) MMDM 1:5.



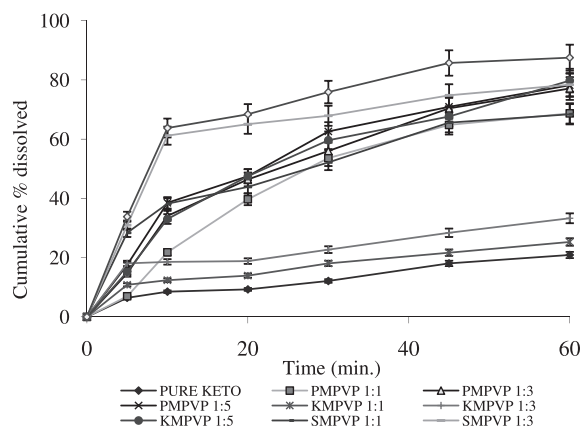
**Figure 6** DSC thermograms of (a) pure drug KETO; (b) PVP K30; (c) PMPVP 1:5; (d) KMPVP 1:5; (e) SMPVP 1:5; (f) D-mannitol; (g) PMDM 1:5; (h) KMDM 1:5 and (i) MMDM 1:5.



**Figure 7** SEM photomicrographs of (a) pure drug KETO (400 $\times$ ); (b) PVP K30 (400 $\times$ ); (c) PMPVP 1:5 (120 $\times$ ); (d) KMPVP 1:5 (200 $\times$ ); (e) SMPVP 1:5 (120 $\times$ ); (f) D-mannitol (400 $\times$ ); (g) PMDM 1:5 (400 $\times$ ); (h) KMDM 1:5 (400 $\times$ ) and (i) MMDM 1:5 (400 $\times$ ).

**Table 2** % Drug dissolved within 30 min ( $DP_{30min}$ ) ( $n = 3$ ).

Sample	$DP_{30min}$ (Mean $\pm$ SD)
Pure KETO	12.11 $\pm$ 0.231
PMPVP 1:1	53.6 $\pm$ 0.467
PMPVP 1:3	56.0 $\pm$ 0.547
PMPVP 1:5	62.6 $\pm$ 0.649
PMDM 1:1	36.64 $\pm$ 0.548
PMDM 1:3	51.62 $\pm$ 0.657
PMDM 1:5	63.76 $\pm$ 0.986
KMPVP 1:1	18.05 $\pm$ 0.675
KMPVP 1:3	22.70 $\pm$ 0.745
KMPVP 1:5	59.63 $\pm$ 0.863
KMDM 1:1	63.80 $\pm$ 0.688
KMDM 1:3	65.82 $\pm$ 0.876
KMDM 1:5	72.28 $\pm$ 1.238
MMDM 1:1	43.4 $\pm$ 0.654
MMDM 1:3	55.23 $\pm$ 0.761
MMDM 1:5	66.34 $\pm$ 0.922
SMPVP 1:1	52.14 $\pm$ 0.542
SMPVP 1:3	67.89 $\pm$ 0.764
SMPVP 1:5	75.89 $\pm$ 0.871

**Figure 8** *In vitro* dissolution profiles of pure KETO and its physical mixtures and solid dispersions with PVP K30 ( $n = 3$ ).

relationship ( $A_L$  type of curve) in the investigated polymer concentration range.

Table 1 shows that all values of  $\Delta G_{tr}^0$  were negative at all levels of carriers, demonstrating spontaneity of drug solubilization process. The values show a declining trend with increase in the carrier concentration too constraining that the process is more favorable at higher carrier levels. Table 1 also indicates that KETO-PVP K30 interaction has a higher  $K_a$  value. The higher  $K_a$  value indicates that the binding affinity between KETO-PVP K30 is more than that of KETO-D-mannitol. The results show that in both cases, the solubility of KETO increased with increasing carrier concentration.

### 3.2. Fourier Transform Infrared Spectroscopy (FTIR) analysis

FTIR spectra of solid dispersions of KETO with PVP K30 and D-mannitol are shown in Figs. 2 and 3, respectively. The spectra of pure KETO presented characteristic peaks at  $1693\text{ cm}^{-1}$  (C=O stretching of acid),  $1655\text{ cm}^{-1}$  (C=O stretching of ketone),  $1598$ ,  $1580$ ,  $1455\text{ cm}^{-1}$  (C=C stretching of aromatic

ring),  $1440\text{ cm}^{-1}$  (C-H deformation of  $\text{CH}_3$  asymmetrical),  $1370\text{ cm}^{-1}$  (C-H deformation of  $\text{CH}_3$  symmetrical), respectively. The characteristic peaks of KETO at  $1693\text{ cm}^{-1}$  (C=O stretching of acid),  $1655\text{ cm}^{-1}$  (C=O stretching of aromatic ring),  $1440\text{ cm}^{-1}$  (C-H deformation of  $\text{CH}_3$  asymmetrical) are also present in spectra of PMPVP 1:5. In the case of KMPVP 1:5 and SMPVP 1:5, a peak at  $1455\text{ cm}^{-1}$  (C=C stretching of aromatic ring) can be assigned for the presence of KETO.

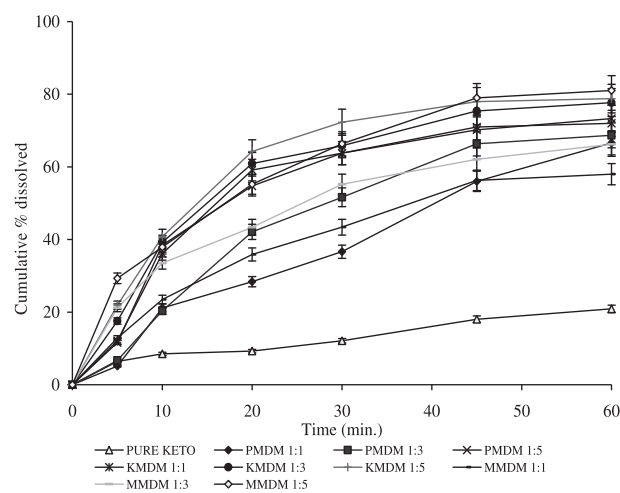
By comparison of spectra of PMDM 1:5, KMDM 1:5, MMDM 1:5, no difference was shown in the position of the absorption bands. Therefore, the spectra can be simply regarded as the superposition of those of KETO and D-mannitol. Therefore, it could be concluded that KETO does not interact with mannitol. Most of the other peaks due to KETO were absent in the spectra of KMPVP 1:5 and SMPVP 1:5 indicating trapping of KETO inside the PVP matrix.

### 3.3. X-ray diffraction (XRD) analysis

Powder XRD of pure KETO, its physical mixtures and solid dispersions with PVP K30 and D-mannitol are shown in Figs. 4 and 5, respectively. The presence of numerous distinct peaks in the X-ray diffraction spectrum indicates that KETO is present as a crystalline material with characteristic diffraction peaks appearing at a diffraction angle of  $2\theta$  at 6.33, 13.16, 14.42, 16.22, 17.30, 18.42, 19.15, 20.04, 22.91, 23.95, 27.23, 27.73, 29.49, etc. Spectroscopy of PVP K30 (Fig. 4b) was characterized by the complete absence of any diffraction peak. PMPVP 1:5, KMPVP 1:5, SMPVP 1:5 (Fig. 4c-e) showed the same diffraction pattern with most of the diffraction peaks corresponding to the drug indicating that KETO was in an amorphous state.

D-Mannitol exhibited a distinct pattern with diffraction peaks (Fig. 5b) at  $2\theta$  at 14.60, 16.78, 18.75, 20.44, 21.06, 23.39, 28.28, 29.48, 31.75, 33.57, 38.72, etc. PMDM 1:5, KMDM 1:5 and MMDM 1:5 showed the presence of characteristic diffraction peaks of both drug and carrier, indicating that KETO was present as crystalline material.

Moreover, no peaks other than those that could be assigned to pure KETO and PVP K30 or D-mannitol were detected in Figs. 4 and 5, respectively.

**Figure 9** *In vitro* dissolution profiles of pure KETO and its physical mixtures and solid dispersions with D-mannitol ( $n = 3$ ).

**Table 3** Similarity factor ( $f_2$ ) for release profiles of KETO from solid dispersions and physical mixtures with PVP K30.

Sample	KETO	SMPVP 1:5	SMPVP 1:3	SMPVP 1:1	KMPVP 1:5	KMPVP 1:3	KMPVP 1:1
KETO	–	11.72	15.27	20.98	19.10	48.23	66.65
PMPVP 1:5	18.30	37.90	–	–	74.42	–	–
PMPVP 1:3	19.53	–	39.95	–	–	25.34	–
PMPVP 1:1	22.87	–	–	47.51	–	–	25.40
KMPVP 1:5	–	35.02	–	–	–	–	–
KMPVP 1:3	–	–	19.07	–	–	–	–
KMPVP 1:1	–	–	–	23.60	–	–	–

### 3.4. Differential Scanning Calorimetry (DSC) analysis

DSC curves obtained for pure KETO, PVP K30, D-mannitol, their physical mixtures and solid dispersions prepared with PVP K30 and D-mannitol, are shown in Fig. 6. Pure powdered KETO thermogram showed a melting endotherm at 92.75 °C with enthalpy of fusion ( $\Delta H$ ) 113.08 J/g. Scanning of PVP K30, a broad endotherm ranging from 80 to 120 °C was observed, because of the presence of residual moisture in PVP K30. The DSC thermogram of PMPVP 1:5 showed a broad peak at 113.53 °C indicating drug amorphization. KMPVP 1:5 and SMPVP 1:5 (Fig. 6d and e) showed broad endotherm due to the presence of water ranging from 80 to 120 °C in PVP K30 and a complete absence of drug peak at 93 °C. This indicates that KETO is present as amorphous or solid solution inside the PVP K30 matrix.

DSC scan of D-mannitol showed single sharp endotherm at 166.29 °C due to melting of D-mannitol, whereas during DSC thermograms of PMDM 1:5, KMDM 1:5, MMDM 1:5 showed the melting peak of the drug at 93 °C and sharp endothermic peak at 166 °C due to the melting of D-mannitol indicating that there is no physical or chemical interaction between KETO and D-mannitol.

### 3.5. Scanning Electron Microscopy (SEM) analysis

SEM photomicrographs obtained for pure KETO, PVP K30, D-mannitol, their physical mixtures and solid dispersions prepared with PVP K30 and D-mannitol, are shown in Fig. 7 in selected magnifications. From the photomicrograph of pure drug KETO, it is clear that the drug was present as irregular shaped crystals. In PMPVP 1:5 and PMDM 1:5, drug particles were adsorbed on the carrier particles. While in the photomicrograph of KMDM 1:5, it can be seen that drug particles are adsorbed on carrier with decreased particle size. This particle size reduction is more efficiently seen with MMDM 1:5. SEM photomicrographs of KMPVP 1:5 and SMPVP 1:5 show

that the drug particles are entrapped within the carrier matrix, confirming FTIR, XRD and DSC data analyses.

### 3.6. *In vitro* dissolution studies

Dissolution of pure KETO and all other prepared systems (solid dispersions and physical mixtures) were carried out in 0.1M HCl.  $DP_{30min}$  (percent drug dissolved within 30 min) values were reported in Table 2. From these data it is evident that the onset of dissolution of pure KETO is very low ( $DP_{30min}$  value 12.11%).

Dissolution profiles of pure KETO, its physical mixtures and solid dispersions with PVP K30 and D-mannitol over a period of 1 h are shown in Figs. 8 and 9, respectively. It can be clearly observed that the dissolution rate of pure KETO is low because 20.89% of drug dissolved in 1 h. Solid dispersions of KETO with PVP K30 and D-mannitol significantly enhanced the dissolution rate of KETO (58–87% with both carriers) within 1 h as compared to physical mixtures as well as pure KETO. Highest improvement was observed in solid dispersions prepared by the solvent evaporation method with PVP K30 (SMPVP 1:5) while in the case of solid dispersions prepared with D-mannitol, the improvement in dissolution rate was higher for MMDM 1:5.

### 3.7. Statistical analysis

Comparisons between the release profiles of KETO from different samples were made by similarity factor  $f_2$ . Calculated  $f_2$  values for PVP K30 and D-mannitol formulations are presented in Tables 3 and 4, respectively.

From Table 3 it is evident that the release profile of KETO from all the samples (i.e., solid dispersions and physical mixtures with PVP K30) and from pure KETO were dissimilar because  $f_2$  values for all comparisons were less than 50 except KMPVP 1:1. Release profiles of KETO from KMPVP and PMPVP at 1:5 ratios were also similar. Table 4 shows that

**Table 4** Similarity factor ( $f_2$ ) for release profiles of KETO from solid dispersions and physical mixtures with D-mannitol.

Sample	KETO	MMDM 1:5	MMDM 1:3	MMDM 1:1	KMDM 1:5	KMDM 1:3	KMDM 1:1
KETO	–	15.97	22.06	27.93	15.14	16.49	18.06
PMDM 1:5	18.29	52.79	–	–	55.18	–	–
PMDM 1:3	22.72	–	53.68	–	–	42.49	–
PMDM 1:1	27.73	–	–	59.63	–	–	35.82
KMDM 1:5	–	62.39	–	–	–	–	–
KMDM 1:3	–	–	47.13	–	–	–	–
KMDM 1:1	–	–	–	39.79	–	–	–

the release profile of KETO from all the samples (i.e., solid dispersions and physical mixtures with D-mannitol) and from pure KETO were dissimilar because  $f_2$  values for all the comparisons were less than 50. But release profiles of KETO from MMDM and PMDM at different ratios, KMDM and PMDM at 1:5 ratios and MMDM and KMDM at 1:5 ratios were similar.

#### 4. Conclusion

From this study, the increase in dissolution rates of KETO, when dispersed in PVP K30 or D-mannitol, can be observed. Solubility studies showed a solubilizing effect of both carriers on KETO. The negative values of Gibbs free energy indicated spontaneity of transfer. XRD, DSC and SEM studies of KETO-PVP K30 solid dispersions indicated that the drug was entrapped within the carrier (PVP K30) matrix while in the case of KETO-D-mannitol mixtures the drug was adsorbed as fine particles on the surface of carrier (D-mannitol). In these systems drug carrier interaction was shown with the use of FTIR. The dissolution rates of physical mixtures were higher than those of pure drug, which was possibly caused by increased drug wettability. Solid dispersions demonstrated higher dissolution rates than physical mixtures. The increased dissolution rates in systems containing D-mannitol were probably the result of decreased particle size, increased wettability and dispersibility of KETO, and in the case of PVP K30 systems that was due to surface tension lowering effect of PVP K30 to the medium, resulting in wetting of hydrophobic and BCS class-II drug (KETO) and thus increase in dissolution rates. SMPVP 1:5 is the best combination for solid dispersions in this study.

#### References

Amidon, G.L., Lennernas, H., Shah, V.P., Crison, J.R., 1995. A theoretical basis for a biopharmaceutical drug classification: the correlation of in vitro drug product dissolution and in vivo bioavailability. *Pharm. Res.* 12, 413–420.

Charman, W.N., 2000. Lipids, lipophilic drugs, and oral drug delivery: some emerging concepts. *J. Pharm. Sci.* 89, 967–978.

Craig, D.Q.M., 1993. The use of self-emulsifying systems as a means of improving drug delivery. In: *Bulletin Technique Gattefosse*, pp. 21–31.

Habib, M.J., 2001. *Pharmaceutical Solid Dispersion Technology*, first ed. Technomic Publishing, Lancaster.

<http://www.fda.gov/downloads/Drugs/GuidanceComplianceRegulatoryInformation/Guidances/ucm070246.pdf> (Accessed on January 21, 2011).

<http://www.fda.gov/downloads/Drugs/GuidanceComplianceRegulatoryInformation/Guidances/ucm070237.pdf> (Accessed on January 21, 2011).

<http://www.tsrlinc.com/resources/services/> (Accessed on January 21, 2011).

Hu, J., Johnston, K.P., Williams III, R.O., 2004. Rapid dissolving high potency danazol powders produced by spray freezing into liquid process. *Int. J. Pharm.* 271, 145–154.

Leuner, C., Dressman, J., 2000. Improving drug solubility for oral delivery using solid dispersions. *Eur. J. Pharm. Biopharm.* 50, 47–60.

Lipinski, C., 2002. Poor aqueous solubility—an industry wide problem in drug delivery. *Am. Pharm. Rev.* 5, 82–85.

Margarit, M.V., Rodriguez, I.C., Cerezo, A., 1994. Physical characteristics and dissolution kinetics of solid dispersions of ketoprofen on polyethylene glycol 6000. *Int. J. Pharm.* 108, 101–107.

Moore, J.W., Flanner, H., 1996. Mathematical comparison of dissolution profiles. *Pharm. Tech.* 20, 64–74.

Roger, J.A., Anderson, A.J., 1982. Physical characteristic and dissolution profiles of ketoprofen-urea solid dispersion. *Pharm. Act. Helv.* 57, 276–282.

Serajuddin, A.T.M., 1999. Solid dispersion of poorly water soluble drugs: early promises, subsequent problems, and recent breakthroughs. *J. Pharm. Sci.* 88, 1058–1066.

Sheen, P.C., Khetarpal, V.K., Cariola, M.C., Rowlings, C.E., 1995. Formulation studies of a poorly water-soluble drug in solid dispersions to improve bioavailability. *Int. J. Pharm.* 118, 221–227.

Takayama, K., Nambu, N., Nagai, T., 1982. Factors affecting the dissolution of ketoprofen from solid dispersions in various water soluble polymers. *Chem. Pharm. Bull.* 3, 3013–3019.

Wyatt, D.A., 1999. Taking poorly water soluble compounds through discovery. In: *Recent Advances in the Formulations and Development of Poorly Soluble Drugs. Bulletin Technique Gattefosse*, pp. 31–39.